

ORIGINAL ARTICLE

# Counter-regulatory phosphatases TNAP and NPP1 temporally regulate tooth root cementogenesis

Laura E Zweifler<sup>1</sup>, Mudita K Patel<sup>1</sup>, Francisco H Nociti Jr<sup>1,2</sup>, Helen F Wimer<sup>3</sup>, Jose L Millán<sup>4</sup>, Martha J Somerman<sup>1</sup> and Brian L Foster<sup>1</sup>

Cementum is critical for anchoring the insertion of periodontal ligament fibers to the tooth root. Several aspects of cementogenesis remain unclear, including differences between acellular cementum and cellular cementum, and between cementum and bone. Biom mineralization is regulated by the ratio of inorganic phosphate ( $P_i$ ) to mineral inhibitor pyrophosphate ( $PP_i$ ), where local  $P_i$  and  $PP_i$  concentrations are controlled by phosphatases including tissue-nonspecific alkaline phosphatase (TNAP) and ectonucleotide pyrophosphatase/phosphodiesterase 1 (NPP1). The focus of this study was to define the roles of these phosphatases in cementogenesis. TNAP was associated with earliest cementoblasts near forming acellular and cellular cementum. With loss of TNAP in the *Alpl* null mouse, acellular cementum was inhibited, while cellular cementum production increased, albeit as hypomineralized cementoid. In contrast, NPP1 was detected in cementoblasts after acellular cementum formation, and at low levels around cellular cementum. Loss of NPP1 in the *Enpp1* null mouse increased acellular cementum, with little effect on cellular cementum. Developmental patterns were recapitulated in a mouse model for acellular cementum regeneration, with early TNAP expression and later NPP1 expression. *In vitro*, cementoblasts expressed *Alpl* gene/protein early, whereas *Enpp1* gene/protein expression was significantly induced only under mineralization conditions. These patterns were confirmed in human teeth, including widespread TNAP, and NPP1 restricted to cementoblasts lining acellular cementum. These studies suggest that early TNAP expression creates a low  $PP_i$  environment promoting acellular cementum initiation, while later NPP1 expression increases  $PP_i$ , restricting acellular cementum apposition. Alterations in  $PP_i$  have little effect on cellular cementum formation, though matrix mineralization is affected. *International Journal of Oral Science* (2014) 7, 27–41; doi:10.1038/ijos.2014.62; published 12 December 2014

**Keywords:** cementum; bone; ectonucleotide pyrophosphatase phosphodiesterase 1; periodontal ligament; progressive ankylosis protein; tissue-nonspecific alkaline phosphatase

## INTRODUCTION

Cementum is a mineralized tissue layer covering the tooth root. Cementum can be categorized into two primary types: acellular cementum (or acellular extrinsic fiber cementum) and cellular cementum (or cellular intrinsic fiber cementum). The thin acellular cementum covers the cervical portion of the tooth root and is critical for anchoring the insertion of periodontal ligament (PDL) fibers. The thicker, bone-like, cellular cementum occupies the apical portion of the root and functions in post-eruption adjustment of tooth occlusion. Several key aspects of cementogenesis remain unclear, including differences between acellular and cellular cementum, and between both types of cementum and bone.<sup>1–4</sup>

Proper regulation of biomineralization is key for formation and function of mineralized tissues. Mineralization is regulated in part by the ratio of inorganic phosphate ( $P_i$ ) to pyrophosphate ( $PP_i$ ) in the extracellular space, as well as other factors including extracellular matrix proteins.  $P_i$  is required for hydroxyapatite crystal initiation and growth, and is dynamically regulated at the systemic and local levels, while  $PP_i$  is

a potent inhibitor of hydroxyapatite crystal growth.<sup>5–8</sup> Local concentration, and thus  $P_i/PP_i$  ratio, is controlled by the activities of various proteins, including phosphatases such as tissue-nonspecific alkaline phosphatase (TNAP, *Alpl*) and ectonucleotide pyrophosphatase phosphodiesterase 1 (NPP1, *Enpp1*), in addition to other regulators.<sup>9</sup>

TNAP is a membrane-bound ectoenzyme that hydrolyzes  $PP_i$ , creating a pro-mineralization milieu.<sup>10</sup> TNAP is expressed by mineralizing cells, e.g. osteoblasts, odontoblasts and chondrocytes. Loss-of-function mutations in the human gene *ALPL* cause hypophosphatasia (HPP), resulting in skeletal and dental hypomineralization.<sup>11–12</sup> The HPP phenotype is recapitulated in the *Alpl*<sup>−/−</sup> mouse model.<sup>13–14</sup> HPP is associated with premature loss of deciduous and permanent teeth, and a mild clinical form of HPP called odontohypophosphatasia features dental defects without skeletal impairment.<sup>15–16</sup> Lack of cementum was found to be the cause of tooth loss in HPP,<sup>17–18</sup> and this phenotype was confirmed in *Alpl*<sup>−/−</sup> mice.<sup>19–20</sup> However, several points about TNAP in relation to cementum formation remain unclear. First, TNAP is rich in the periodontal region in PDL and gingiva, as well as the surrounding bone,

<sup>1</sup>National Institute of Arthritis and Musculoskeletal and Skin Diseases (NIAMS), National Institutes of Health (NIH), Bethesda, USA; <sup>2</sup>Department of Prosthodontics and Periodontics, Division of Periodontics, School of Dentistry, Campinas State University, Piracicaba, Brazil; <sup>3</sup>Department of Vertebrate Zoology, National Museum of Natural History, Smithsonian Institution, Washington, USA and <sup>4</sup>Sanford Children's Health Research Center, Sanford-Burnham Medical Research Institute, La Jolla, USA  
Correspondence: Dr BL Foster, National Institutes of Arthritis and Musculoskeletal and Skin Diseases (NIAMS), National Institutes of Health (NIH), Building 50/Room 4120, Bethesda MD 20892, USA  
E-mail: brian.foster@nih.gov  
Accepted 6 August 2014

yet some studies have suggested cementoblasts do not express TNAP.<sup>21</sup> In such an alkaline phosphatase-rich environment, is TNAP expression required of cementoblasts to promote cementum mineralization? Secondly, in the alkaline phosphatase-rich periodontal region, how is it that the PDL does not progressively mineralize to produce ankylosis of tooth to bone? Do cementoblasts developmentally regulate TNAP expression to prevent cementum overgrowth? Thirdly, while acellular cementum formation is inhibited in HPP, cellular cementum has been described frequently as unaffected or less affected. Is there a different functional importance for TNAP in acellular *vs.* cellular cementum formation?

The nucleotide pyrophosphatase phosphodiesterase (NPP) family is comprised of seven isozymes, NPPs 1–7.<sup>22–24</sup> NPP1 is an ectoenzyme that converts extracellular nucleotides (such as ATP) to PP<sub>i</sub>.<sup>25</sup> By increasing local PP<sub>i</sub>, NPP1 activity regulates mineralization by antagonizing PP<sub>i</sub> hydrolysis by TNAP.<sup>9,26–27</sup> Loss-of-function of NPP1 underlies calcification disorders including generalized arterial calcification of infancy.<sup>28</sup> The *Enpp1*<sup>-/-</sup> mouse model presents hypermineralization of joints and articular cartilages.<sup>26–27,29</sup> *Enpp1*<sup>-/-</sup> mice feature rapidly forming acellular cementum, reflecting the PP<sub>i</sub> poor environment.<sup>19,30</sup> However, questions remain regarding the precise function of NPP1 in cementogenesis. For example, how does the developmental expression pattern of NPP1 reflect its role in acellular *versus* cellular cementum formation? Also, do related proteins such as NPP2 or NPP3 have roles in tooth mineralization, and are they capable of compensating for the absence of NPP1?

Our current studies were targeted at better defining the roles of phosphatases TNAP and NPP1 in cementogenesis. To address the questions outlined above, and consider how these factors coregulate cementum formation, we analyzed spatiotemporal expression patterns of TNAP and NPP1 using mouse models, examined effects of ablating these factors with a focus on acellular *versus* cellular cementum types, and determined gene and protein expression patterns in mineralizing cementoblasts *in vitro*. We assessed expression of these two factors during wound healing and neocementogenesis in a rodent periodontal defect model, and compared findings in mice to expression patterns in normal human tissues.

## MATERIALS AND METHODS

### Mouse and human samples used for histology

Generation and genotyping of mouse models were described previously for *Alpl*<sup>-/-</sup> mice,<sup>14</sup> *Enpp1*<sup>-/-</sup> mice<sup>27</sup> and *Ank*<sup>-/-</sup> mice.<sup>31</sup> At developmental ages of interest (4, 8, 14, 26 and 60 days post-natal; dpn), mandibles were harvested and fixed in Bouin's solution. Human samples included de-identified teeth extracted for orthodontic reasons, and use of discarded dental tissues was approved for exemption by the Human Subjects IRB at the National Institutes of Health (Bethesda, MD, USA). Human teeth were fixed in 10% neutral buffered formalin. Samples for histology were demineralized in AFS (acetic acid, formaldehyde and sodium chloride) and embedded in paraffin for serial sectioning, as described previously.<sup>32</sup>

### Undecalcified histology

Tissues used for undecalcified sectioning were fixed in paraformaldehyde and embedded in methylmethacrylate and stained by von Kossa and Goldner's trichrome stains, as described previously.<sup>33</sup>

### Immunohistochemistry

Immunohistochemistry was performed as described previously.<sup>32</sup> Species-specific biotinylated secondary antibodies were used to localize an avidin-enzyme complex to antigens, and a 3-amino-9-ethylcarbazole

substrate kit was used to produce a red product (Vector Labs, Burlingame, CA, USA). Three TNAP antibodies were tested with similar results, and representative reactions from rat monoclonal immunoglobulin G (IgG) anti-human ALPL (R&D Systems, Minneapolis, MN, USA) are shown, and have been validated previously.<sup>19,33–36</sup> Additional TNAP antibodies included goat polyclonal anti-mouse ALPL antibody (R&D Systems) and rabbit polyclonal anti-mouse ALPL antibody (Abcam, Cambridge, MA, USA). TNAP immunohistochemistry included antigen retrieval by overnight incubation at room temperature in 8 mol·L<sup>-1</sup> guanidine hydrochloride (pH 8.5). Goat polyclonal IgG anti-human NPP1 antibody (Abcam, Cambridge, MA, USA) was used and has been reported previously.<sup>19,37</sup> Rabbit polyclonal IgG anti-human NPP2 antibody (Abcam, Cambridge, MA, USA) was used with heat-mediated antigen retrieval citrate buffer (pH 6.0) solution, per manufacturer's (Abcam, Cambridge, MA, USA) instructions. Rabbit polyclonal IgG anti-human NPP3 antibody (Abcam, Cambridge, MA, USA) was used.

### Tissue-specific gene expression analysis

Total RNA was isolated from CD-1 mouse tissues at 8 and 15 dpn (early and later tooth root developmental stages) for gene expression analysis. Tissues included molar teeth, femurs, calvarias and brains (*n*=3–6 for each). Tissues were pulverized with mortar and pestle in liquid nitrogen under RNase-free conditions. Trizol reagent (Life Technologies, Grand Island, NY, USA) was used to isolate total RNA, then transcribed to cDNA (Transcriptor Kit; Roche Applied Sciences, Indianapolis, IN, USA) for quantitative real-time polymerase chain reaction (PCR) analysis (LightCycler 480 II; Roche Diagnostics GmbH, Mannheim, Germany). Gene-specific primers for *Alpl*, *Enpp1*, *Enpp2*, *Enpp3* and glyceraldehyde-3-phosphate dehydrogenase (*Gapdh*; house-keeping gene) are listed in Supplementary Table S1. Techniques have been described previously.<sup>37</sup>

### Microcomputed tomography

Microcomputed tomography (microCT) analysis of *Alpl* mouse mandibles was performed using a Skyscan model 1076 microtomograph (Skyscan, Kontich, Belgium). Scanning was performed under the following parameters: 9 micron voxel resolution, 65 kV, 150 μA, and with a 1.0 mm Al filter. Cut planes of mandibles were created using CTan software (Skyscan, Kontich, Belgium).

### Periodontal defect model

The surgical periodontal defect model has been described for rats,<sup>38</sup> and we employed a similar approach for mice, removing cementum from the buccal root surfaces of the distal root of the first mandibular molar and mesial root of the second molar.<sup>39</sup> Wild-type (WT) mice at 5 weeks of age underwent surgery to create a periodontal defect (2 mm in length, 1 mm in width and 0.5 mm in depth) on the buccal bone, removing cementum from the distal root of the first mandibular molar and mesial root of the second molar. Mandibles were harvested for analysis at 1, 15 and 30 days post-surgery.

### Cell culture

OCCM.30 immortalized mouse cementoblasts have been described previously.<sup>40–41</sup> Cells were maintained in Dulbecco's modified Eagle medium (DMEM) with 10% fetal bovine serum and 1% PSG (penicillin, streptomycin and glutamine). For mineralization experiments, cells were plated at a concentration of 2.1×10<sup>4</sup> cells per cm<sup>2</sup> and provided with 2% fetal bovine serum in DMEM and 50 μg·mL<sup>-1</sup> ascorbic acid (non-mineralizing conditions), or with addition of organic P<sub>i</sub> source, 10 mmol·L<sup>-1</sup> β-glycerophosphate (BGP), to establish mineralizing conditions. Media were changed every two days. Cell culture experiments were performed four times in triplicate.

Total RNA was collected from cells on days 1, 3, 5, 7, 9 and 11, following manufacturer's instructions (Qiagen, Valencia, CA, USA). RNA was used to synthesize cDNA for quantitative real-time PCR (described above). Total cellular protein was collected using a mammalian protein extraction reagent kit following manufacturer's instructions (Thermo Fisher Scientific, Rockford, IL, USA). Protein samples were stabilized with protease inhibitor cocktail (Thermo Fisher Scientific, Rockford, IL, USA). Concentrations of TNAP, NPP1, NPP2 and NPP3 in cell cytoplasm and membrane fractions were measured using enzyme linked immunosorbent assay (ELISA) kits with specificity for mouse (MyBioSource, San Diego, CA, USA).

Mineralization by OCCM.30 cells *in vitro* was determined on days 4, 6, 8, 10 and 12. The qualitative von Kossa stain was performed to visualize mineral nodule formation, as described previously.<sup>19</sup> Cells were fixed in 100% ethanol and rehydrated in a descending ethanol series. After being incubated with 5% AgNO<sub>3</sub> solution at 37 °C for 1 h, plates were rinsed several times with water and placed on a light box. Mineral nodules were indicated by silver deposits that appeared as dark brown-black staining in the fixed matrix layer.

A quantitative calcium assay was also used to assess *in vitro* mineralization, as described previously.<sup>19</sup> Cells were fixed and rehydrated as described above for the von Kossa assay. After incubation in a 0.5 mol·L<sup>-1</sup> HCl solution, a calcium reagent (Genzyme Diagnostics, Charlottetown, Prince Edward Island, Canada) was used to quantify calcium based on a standard curve of known concentrations, with absorbance measured at 650 nm.

### Statistical analysis

Intergroup mean differences were analyzed by Student's (independent samples) *t*-test or one-way analysis of variance (ANOVA) using GraphPad Prism 6.01 (GraphPad Software, San Diego, CA, USA). Data are presented as means ± standard deviation, where significant differences are achieved at *P* < 0.05.

## RESULTS

### Tissue specific gene expression analysis

Messenger RNA (mRNA) expression levels of phosphatases of interest were analyzed by quantitative PCR using mouse tissues harvested at 8 dpn. Molars were compared to femur and calvarial bone, and to brain as a control non-mineralizing tissue. Molars featured significantly higher expression of *Alpl*, *Enpp2* and *Enpp3* vs. other tissues (Supplementary Figure S1). Molars and femurs expressed significantly higher levels of *Enpp1* vs. brain, with calvaria not significantly different compared to other tissues. Similar trends were observed in 15 dpn tissues (data not shown). Based on the robust expression of these factors during tooth formation, we analyzed the spatiotemporal expression of these four phosphatases in tooth development.

### Developmental pattern and functional analysis of TNAP in cementum formation

It is established that TNAP is expressed in the periodontium and is associated with cementum formation.<sup>19,42–44</sup> Furthermore, TNAP is required for proper formation of the acellular cementum, as demonstrated in *Alpl*<sup>-/-</sup> mouse models,<sup>19,20,45</sup> and loss-of-function of TNAP causes premature tooth loss in hypophosphatasia (HPP).<sup>16,18,46</sup> However, some aspects of TNAP function in cementogenesis remain unclear, and here we performed a careful spatiotemporal analysis of developmental expression of TNAP in order to refine our understanding of the role of TNAP in root formation.

Prior to onset of cementogenesis in first molars at 4 and 8 dpn, TNAP was expressed in odontoblasts and in osteoblasts of the surrounding alveolar bone (Figure 1a–1d), as described previously.<sup>35–36</sup> At both these ages, the dental follicle, precursor to the PDL and containing cementoblast precursors, was notably negative for TNAP localization. A more developmentally advanced 8 dpn molar root exhibited the first sign of positive TNAP staining in the dental follicle, where acellular cementum formation was initiating (Figure 1e). Interestingly, staining at 8 dpn revealed a burst of TNAP expression in the cervical-most ameloblasts (star in Figure 1e), at a position near where a unique type of cementum with unknown origin and function, the acellular afibrillar cementum, forms.<sup>47–48</sup> At the more advanced stage of root formation at 14 dpn, TNAP was widely expressed in the PDL, including in cementoblasts on the cervical root surface (Figure 1f). In the apical root tip, TNAP positive cells (putative cementoblasts) were visible near the root surface only after separation of HERS from the root (Figure 1g). At 26 dpn, TNAP localization remained strong in the PDL, including in cells surrounding the forming cellular cementum (Figure 1h–1i). The presence of TNAP remained widespread in the molar periodontium at 60 dpn (Figure 1j).

The mouse continuously growing incisor features acellular cementum on the root analog of the lingual surface. Unlike the molar, where TNAP became ubiquitous in the organized PDL (14 dpn and older in Figure 1), the mouse incisor featured a distinct pattern of restricted TNAP expression around the tooth at all ages observed (Supplementary Figure S2a–S2c). A sagittally sectioned incisor was employed to analyze TNAP expression over the course of incisor maturation from the apical (immature) origin to the incisal (mature) edge (Supplementary Figure S2d). TNAP expression within the PDL was greatest near the alveolar bone (Supplementary Figure S2e–S2g). TNAP expression near the incisor root was greatest in the apical portion, coincident with acellular cementum initiation (Supplementary Figure S2g), and TNAP expression became further removed from the tooth surface as the incisor grew outward (Supplementary Figure S2e and S2f), *i.e.*, TNAP expression was disassociated from more mature cementum in the incisor tooth.

Developmental analysis of TNAP expression (Figure 1 and Supplementary Figure S2) indicated direct association of TNAP with initiation of cementum. Previously, it has been shown that TNAP is required for proper formation of acellular cementum, as demonstrated in *Alpl*<sup>-/-</sup> mouse models,<sup>19–20,45</sup> and in human cases of HPP.<sup>16,18,46</sup> To further clarify the roles of TNAP in acellular and cellular cementum formation, we further analyzed root formation in the *Alpl*<sup>-/-</sup> mouse model.

Compared to WT mouse molars at 14 dpn, where TNAP was localized to PDL and cementoblasts, *Alpl*<sup>-/-</sup> molars lacked acellular cementum and featured large regions of hypomineralized root dentin (Figure 2a–2d). Inhibition of acellular cementum was also observed on *Alpl*<sup>-/-</sup> incisors (data not shown). By 20 dpn, WT molars were forming cellular cementum on the apical portion (Figure 2e and 2f). Surprisingly, in contrast to acellular cementum, *Alpl*<sup>-/-</sup> mouse molars featured an enlarged cellular cementum-like layer covering a larger and more cervical region of the root compared to WT, and adjacent to hypomineralized root dentin (Figure 2g and 2h). The composition of the larger cellular cementum layer on *Alpl*<sup>-/-</sup> mouse molars appeared similar to WT by picosirius red stain under polarized light, featuring red-stained, loose packed collagen fibers (Figure 2i–2l). The mineralized status of root dentin and cellular cementum of WT molars was shown by von Kossa and Goldner trichrome staining, and microCT scanning, whereas *Alpl*<sup>-/-</sup> cellular cementum and underlying root dentin were severely hypomineralized

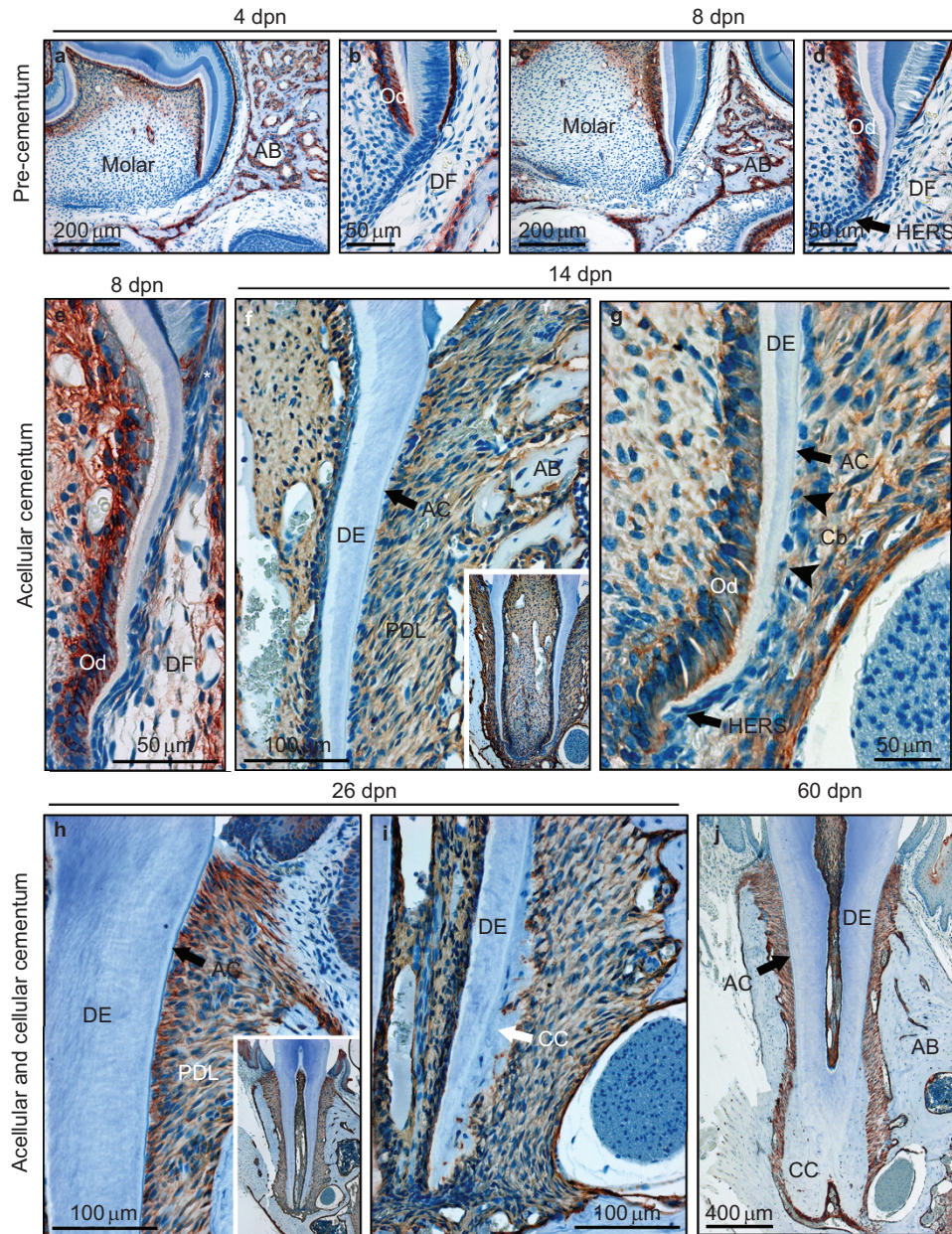


**Figure 1** Developmental expression of TNAP during molar root formation. Prior to onset of cementogenesis in first molars at (a, b) 4 dpn and (c, d) 8 dpn, TNAP is expressed in Ods and osteoblasts of the surrounding AB, as well as in stratum intermedium of the enamel organ. Note the lack of TNAP in the DF at both these ages. (e) In another 8 dpn molar, more advanced in root formation than that shown in c and d, cells near the outer root surface begin to exhibit TNAP where AC will form. Note the burst of TNAP expression in the cervical most ameloblasts (indicated by \*), at a position near where AAC forms in some teeth. (f) As root formation progresses at 14 dpn, TNAP is expressed strongly in the PDL, including in the cementoblast cell layer bordering the root surface. (g) In the apical root, TNAP positive cells (arrowheads indicating Cbs) are visible approaching the root surface after separation of HERS from the root surface. (h) TNAP localization remains strong in the PDL of the mature tooth at 26 dpn. (i) During formation of CC, TNAP is expressed in associated cementoblasts. (j) TNAP expression remains strong at 60 dpn, even after the molar tooth has been completed and in occlusion for more than one month. AAC, acellular afibrillar cementum; AB, alveolar bone; AC, acellular cementum; Cb, cementoblast; CC, cellular cementum; DF, dental follicle; dpn, days post-natal; HERS, Hertwig's epithelial root sheath; Od, odontoblast; PDL, periodontal ligament; TNAP, tissue-nonspecific alkaline phosphatase.

(Figure 2m–2p). The larger and more cervically located cellular cementum of the *Alpl*<sup>-/-</sup> molars therefore was confirmed to be unmineralized cementoid. Advanced ages of *Alpl*<sup>-/-</sup> mice could not be studied due to the early lethality of these mice.

#### Developmental pattern and functional analysis of NPP1 in mouse cementum formation

As TNAP functions in skeletal mineralization by reducing PP<sub>i</sub>, NPP1 is hypothesized to play an antagonistic role by increasing extracellular

PP<sub>i</sub>.<sup>9,26,27</sup> While it is known that NPP1 is involved in regulating acellular cementum growth,<sup>19,30</sup> a detailed expression pattern of NPP1 during tooth development has not been reported, and was performed first, followed by analysis of *Enpp1*<sup>-/-</sup> mice over a range of ages not previously published.

In parallel to TNAP, we mapped NPP1 expression during tooth root formation. Because of the relatively low expression of NPP1 throughout tooth formation, as an additional illustrative example, we employed an *Ank*<sup>-/-</sup> mouse model, which is hypermineralizing and

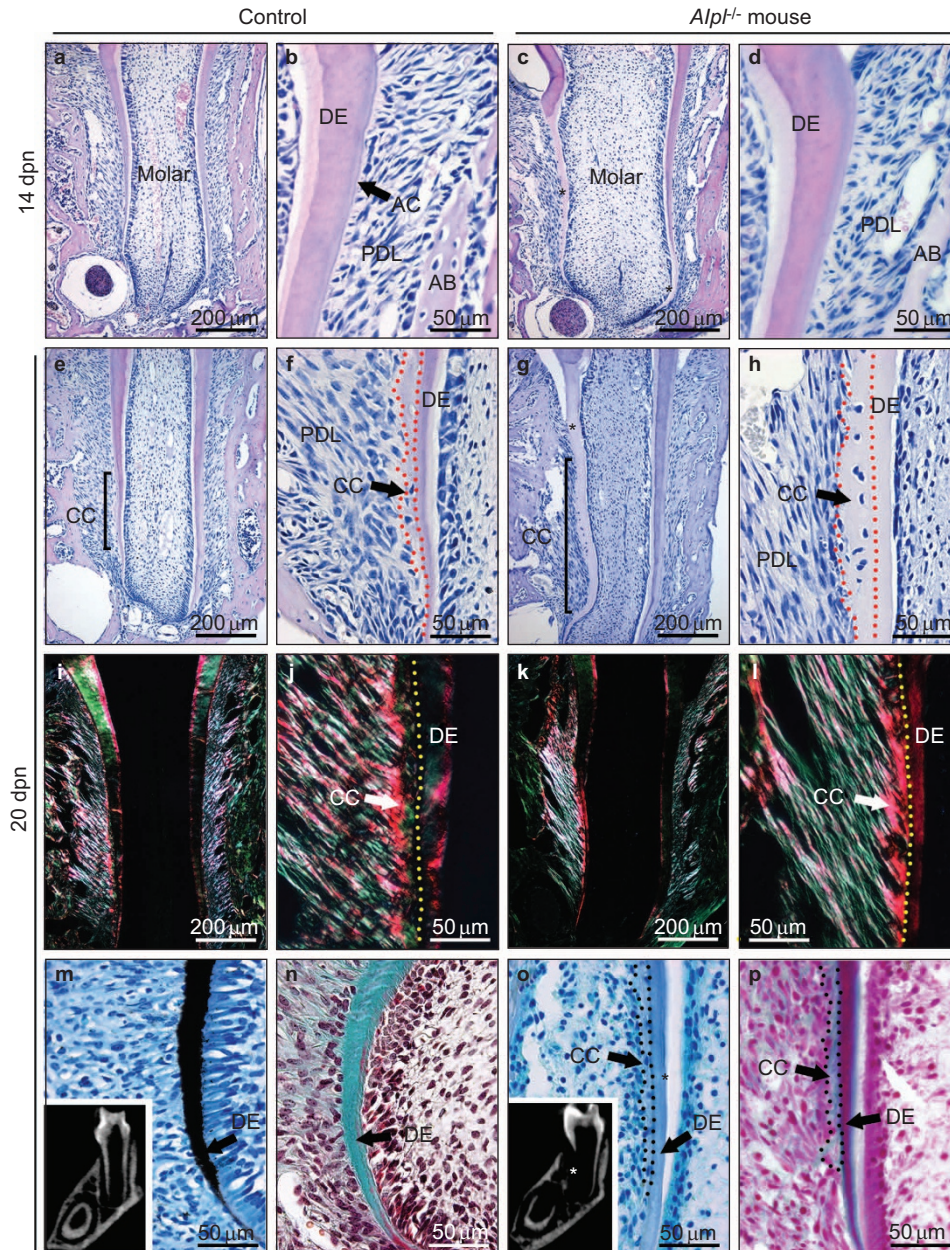


**Figure 2 TNAP is required for proper cementum mineralization.** Compared to (a, b) WT mouse molars at 14 dpn, (c, d) *Alpl*<sup>-/-</sup> mouse molars lack AC and also feature large regions of unmineralized (\*) root DE. By the later age of 20 dpn, (e, f) WT molars form CC on the apical-most portion of the molar. (g, h) *Alpl*<sup>-/-</sup> mouse molars at 20 dpn feature a thicker cellular cementum-like layer covering a larger and more cervical region of the root, in relation to severely hypomineralized root dentin (indicated by \*). (i–l) The larger cellular cementum layer (to the left of the yellow dotted line) of the *Alpl*<sup>-/-</sup> mouse features red-stained, loose packed collagen fibers, similar to WT, under polarized light. The root dentin and cellular cementum of WT molars are well mineralized, as determined by (m) von Kossa stain, microCT (inset) and (n) Goldner trichrome stain, while (o–p) *Alpl*<sup>-/-</sup> cellular cementum and underlying root dentin are confirmed to be hypomineralized using the same methods (indicated by \* in microCT panel in o). In o–p, the thickened cellular cementum is outlined in black dotted lines, whereas no equivalent cellular cementum layer is yet evident on the WT molars in m and n. AC, acellular cementum; CC, cellular cementum; DE, dentin; dpn, days post-natal; microCT, microcomputed tomography; TNAP, tissue-nonspecific alkaline phosphatase; WT, wild-type.

over-expresses NPP1 compared to controls.<sup>19</sup> NPP1 localization was not observed in the molar or incisor at the early age of 4 dpn (data not shown). At 8 dpn, at the earliest initiation of cementogenesis, NPP1 was not detected around the tooth root (Figure 3a and 3b). In contrast, the 8 dpn *Ank*<sup>-/-</sup> molar featured abundant NPP1 expression in cells along the root surface, where acellular cementum was visibly wider compared to WT, showing that accelerated acellular cementum

formation spurred early and increased NPP1 in cementoblasts (Figure 3c). At 14 dpn, NPP1 was localized to cementoblasts near the cervical root (where acellular cementum was oldest and thickest), but not detectable in the most apical root where new acellular cementum was initiating (Figure 3d and 3f). The 14 dpn *Ank*<sup>-/-</sup> molar featured robust NPP1 over-expression in cementoblasts along the entire acellular cementum (Figure 3g). In the completed molar at

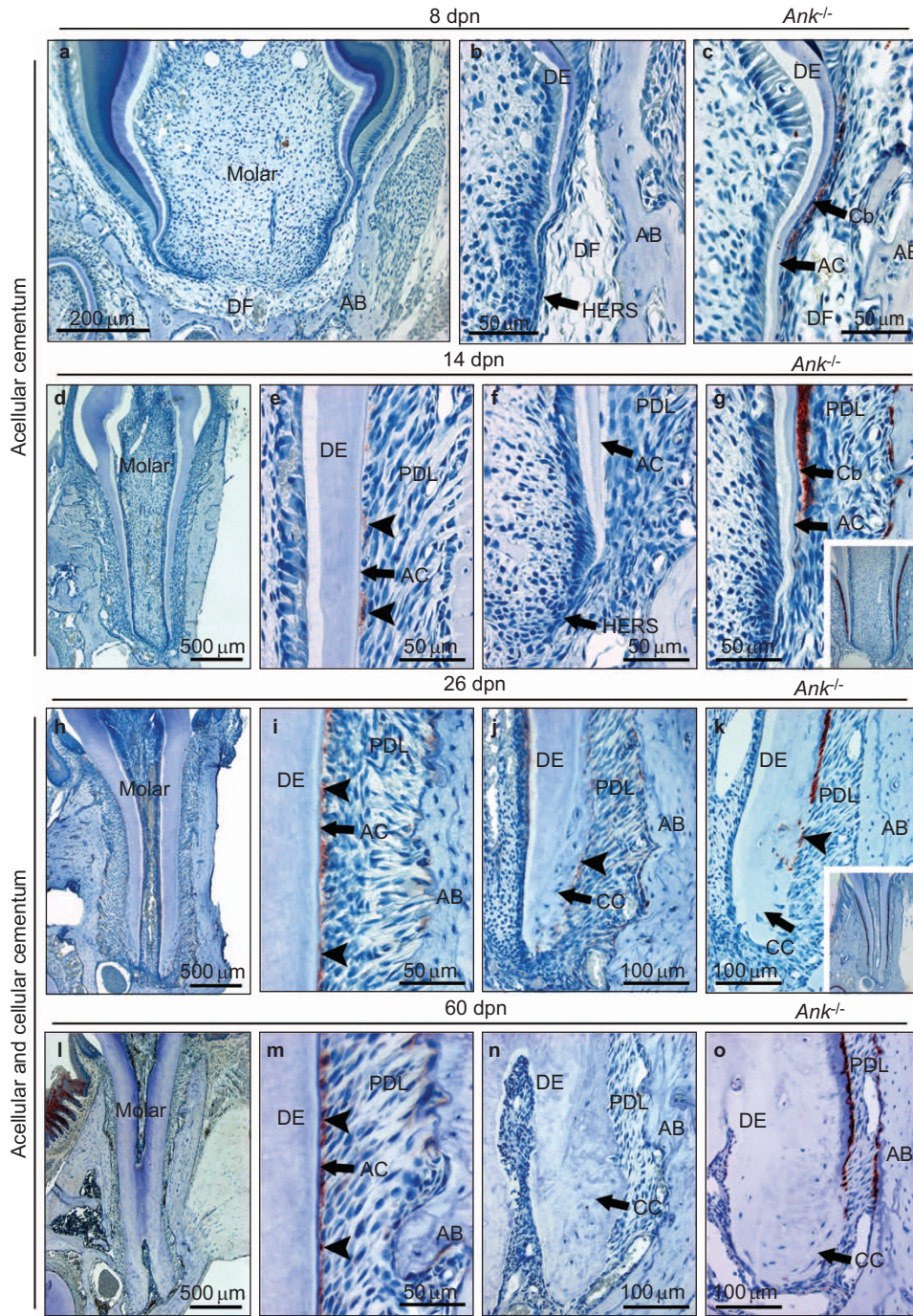


**Figure 3** Developmental expression of NPP1 during molar root formation. (a, b) At 8 dpn, at the earliest initiation of cementogenesis, NPP1 is not detected around the tooth root, in the DF or AB. (c) In the hypermineralizing *Ank*<sup>-/-</sup> mouse, Cb express NPP1 along the root surface adjacent to thicker AC, though increased NPP1 is not detected elsewhere. (d, e) At 14 dpn, NPP1 is localized to some cementoblasts (arrowheads) near the cervical root (where acellular cementum is oldest and thickest), but not detectable in (f) the most apical portion of the root where acellular cementum mineralization initiates following break-up of HERS. (g) The *Ank*<sup>-/-</sup> molar at 14 dpn features robust NPP1 over-expression in cells along the entire acellular cementum surface. (h, i) In the mature molar at 26 dpn, NPP1-positive cells (arrowheads in i) line the acellular cementum-covered cervical root, and (j) NPP1 is found in scattered cementoblasts of the apical CC. (k) The *Ank*<sup>-/-</sup> molar at 26 dpn features increased NPP1 staining in cementoblasts (arrowheads) along the thick acellular cementum, though the cellular cementum does not exhibit more staining than WT. (l) NPP1 expression patterns remain similar at 60 dpn, with consistent localization to (m) cementoblasts of the acellular cementum, but less so in cells of the (n) cellular cementum. (o) *Ank*<sup>-/-</sup> molars maintain high NPP1 expression in cementoblasts lining the acellular cementum, with less staining around cellular cementum. AB, alveolar bone; AC, acellular cementum; Cb, cementoblast; CC, cellular cementum; DE, dentin; DF, dental follicle; dpn, days post-natal; HERS, Hertwig's epithelial root sheath; NPP, nucleotide pyrophosphatase phosphodiesterase; PDL, periodontal ligament; WT, wild-type.

26 dpn, NPP1 lined the acellular cementum-covered cervical root, and was minimally expressed in cells by the apical cellular cementum (Figure 3h–3j). While the *Ank*<sup>-/-</sup> acellular cementum featured abundant NPP1 staining, the cellular cementum was not different than WT (Figure 3k). These patterns were maintained at age 60 dpn (Figure 3l–3o), where NPP1 was found some limited regions of *Ank*<sup>-/-</sup> alveolar bone where an overgrown layer similar in appearance to acellular cementum was present on the bone surface (Figure 3o).

Parallel to the molar teeth, the incisor featured no detectable NPP1 at 8 dpn (closer to cementum initiation), but NPP1 expression was found specifically in cementoblasts at later ages of 14 and 26 dpn, after acellular cementum was established (Supplementary Figure S3a–S3c).

The *Ank*<sup>-/-</sup> incisor featured marked staining for NPP1 along the surface of increased cementum at all these ages (Supplementary Figure S3a–S3c, insets). Employing a sagittal section of the incisor revealed that NPP1 expression was not found in the apical portion, but increased in cementoblasts of the middle and incisal portions, following acellular cementum formation (Supplementary Figure S3d–S3g). NPP1 was also identified in the PDL region in the incisal portion (Supplementary Figure S3e).

Next, we analyzed the loss of NPP1 in light of its developmental expression. At 14 dpn, where NPP1 was first detected along the acellular cementum of the molar, the *Enpp1*<sup>-/-</sup> mouse exhibited several-fold thicker cementum compared to WT (Figure 4a–4d). At 26 dpn, the

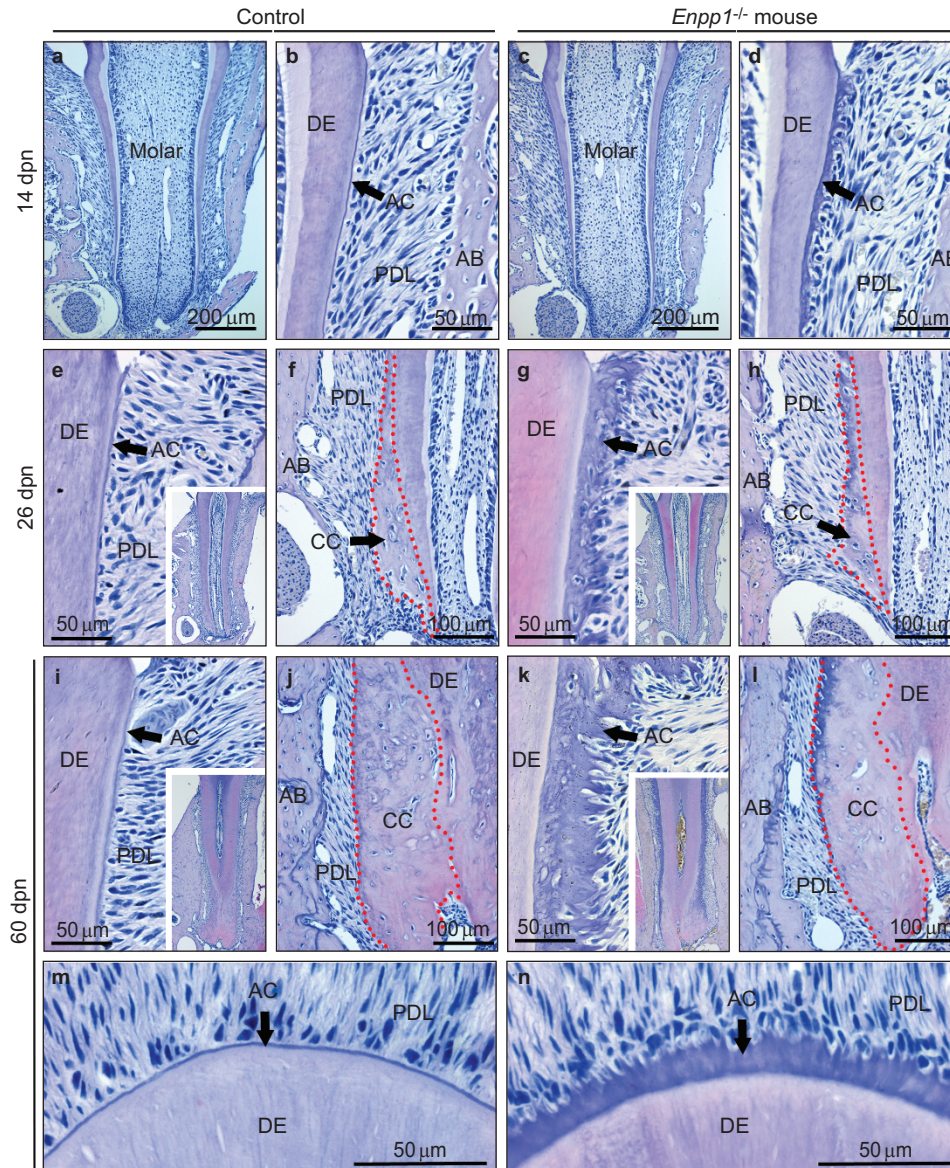


**Figure 4 Role of NPP1 in regulating cementum apposition.** Compared to (a, b) WT mouse molars at 14 dpn, (c, d) *Enpp1*<sup>-/-</sup> mouse molars exhibit several-fold thicker AC. (e) Compared to the slow acellular cementum growth in WT molars by 26 dpn, (g) *Enpp1*<sup>-/-</sup> molars feature rapidly increasing acellular cementum, approximately 30–40 μm at this stage. At 26 dpn, the CC does not appear different between (f) WT and (h) *Enpp1*<sup>-/-</sup> molars. (i, k) By 60 dpn, acellular cementum in the *Enpp1*<sup>-/-</sup> mouse measure more than 50 μm, compared to 5 μm in the WT, and (j, l) cellular cementum appears similar between them. (m, n) *Enpp1*<sup>-/-</sup> incisors feature increased cementum in parallel to molars. AB, alveolar bone; AC, acellular cementum; CC, cellular cementum; DE, dentin; dpn, days post-natal; NPP, nucleotide pyrophosphatase phosphodiesterase; PDL, periodontal ligament; WT, wild-type.

*Enpp1*<sup>-/-</sup> mouse molar acellular cementum had expanded rapidly, measuring 30–40  $\mu\text{m}$  in thickness compared to 3–4  $\mu\text{m}$  in WT, though cellular cementum appeared unaltered (Figure 4e–4h). By 60 dpn, acellular cementum in the *Enpp1*<sup>-/-</sup> mouse measured more than 50  $\mu\text{m}$ , compared to 5  $\mu\text{m}$  in the WT, and cellular cementum appeared no different between them (Figure 4i–4l). The *Enpp1*<sup>-/-</sup> incisor tooth featured substantially increased acellular cementum in parallel to the molar (Figure 4m and 4n).

### Developmental expression of NPP2 and NPP3 in mouse cementum formation

The importance of NPP1 in cementum formation, based on developmental expression and loss-of-function analysis, prompted us to explore the potential roles of NPP2 and NPP3 in cementum mineralization. NPP2 and 3 were localized in tooth and periodontal tissues by immunohistochemistry over the course of development, and representative 60 dpn sections are shown in Figure 5. NPP2 expression

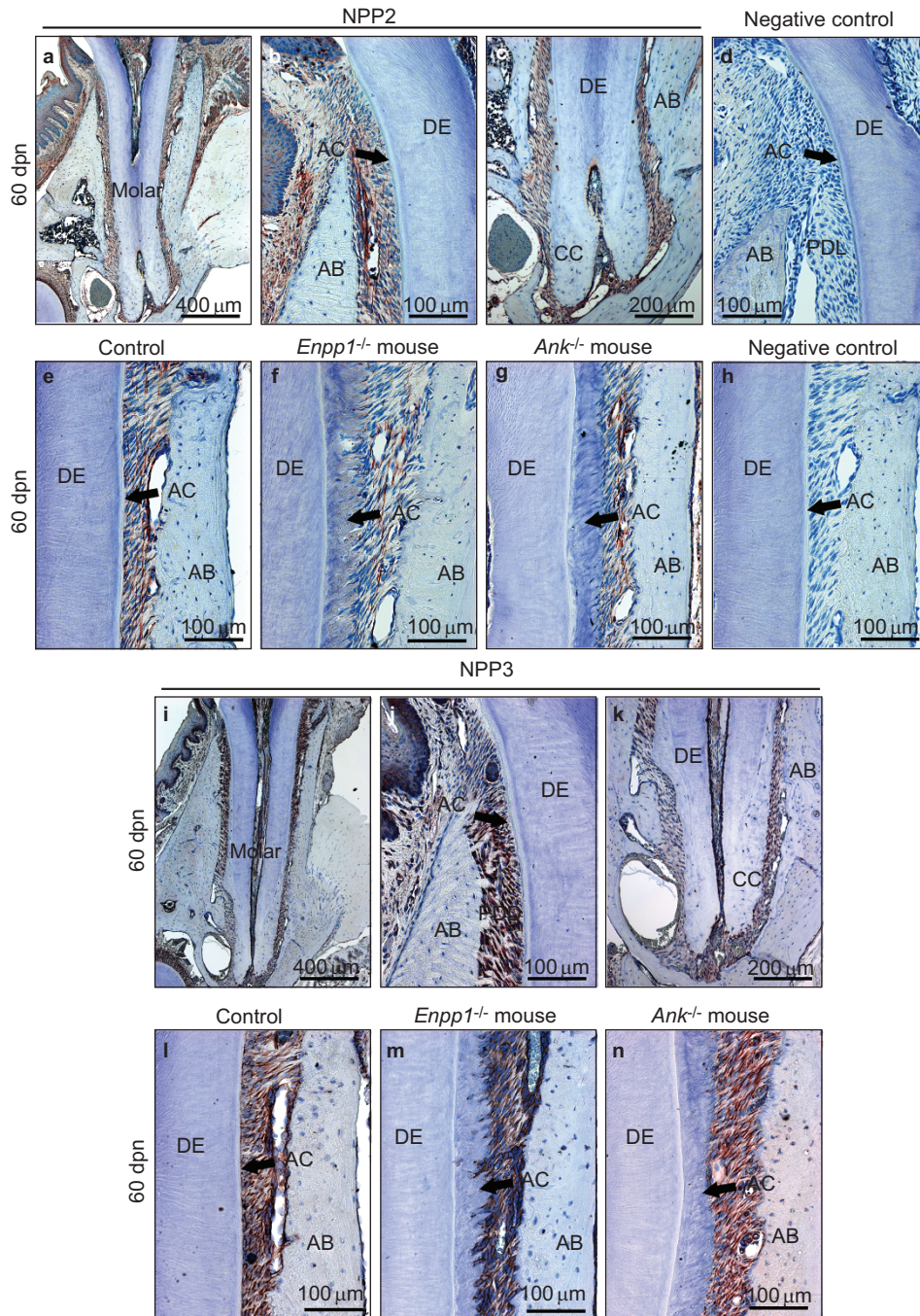


**Figure 5** Expression of NPP2 and 3 in the periodontium. (a–c) At 60 dpn, NPP2 expression is expressed widely in the pulp–dentin complex and periodontium of the mandibular first molar, including in cementoblasts near the cervical and apical root. (e–g) NPP2 expression and localization are not altered in *Ank*<sup>-/-</sup> nor *Enpp1*<sup>-/-</sup> mice compared to WT controls. (i–k) NPP3 is expressed widely in the tooth and surrounding periodontal tissues, including cementoblasts near acellular and cellular cementum. (l–n) Expression and localization patterns of NPP3 in the periodontia are not altered in *Ank*<sup>-/-</sup> or *Enpp1*<sup>-/-</sup> mice compared to WT controls. Negative controls (d, h) included no primary antibody. AB, alveolar bone; AC, acellular cementum; CC, cellular cementum; DE, dentin; dpn, days post-natal; NPP, nucleotide pyrophosphatase phosphodiesterase; PDL, periodontal ligament; WT, wild-type.

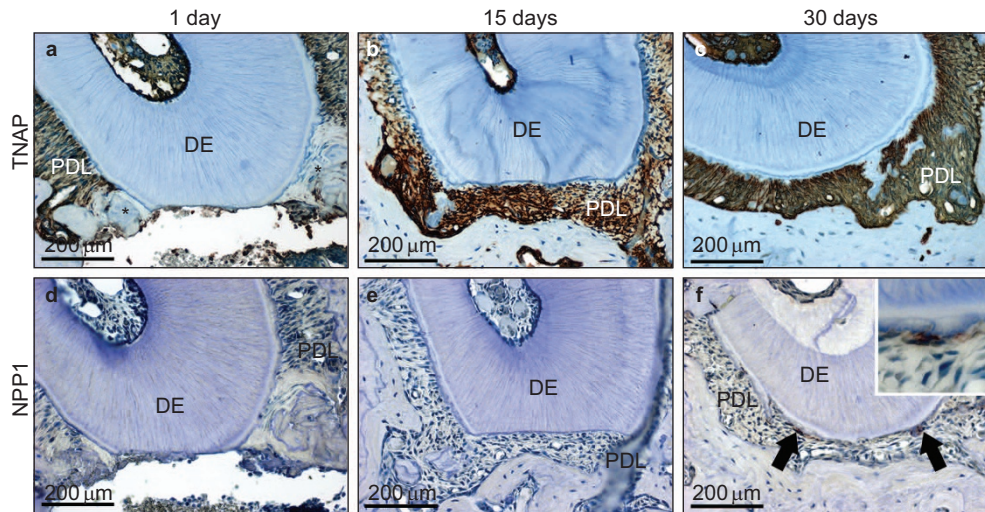


**Figure 6** Expression of TNAP and NPP1 in cementum regeneration. A 1 mm×2 mm window in alveolar bone was created to remove cementum and superficial DE from the buccal root surfaces of the distal root of the first mandibular molar and mesial root of the second molar in 4-week-old mice. (a) At 1 day post-surgery, loose granulation tissue surrounds the cementum defect, with no detectable TNAP localization (\*), though TNAP was localized to the larger PDL region away from the wound. (b) By day 15, strong localization of TNAP along the root surface accompanies the formation of new cementum, and (c) TNAP returns to its normal ubiquitous pattern in the healed PDL by 30 days. (d–f) NPP1 was not detectable along the root surface until the advanced time point of 30 days, after new cementum formation, when NPP1-positive cementoblast cells are visible (black arrows in f). DE, dentin; NPP, nucleotide pyrophosphatase phosphodiesterase; PDL, periodontal ligament; TNAP, tissue-nonspecific alkaline phosphatase.

was widely detected in the pulp–dentin complex as well as the periodontium (Figure 5a), including in cementoblasts (Figure 5b and 5c). Widespread expression of NPP2 has been reported in other tissues.<sup>49</sup> Compared to WT, neither *Ank*<sup>-/-</sup> nor *Enpp1*<sup>-/-</sup> mice featured altered NPP2 in response to low PP<sub>i</sub> and hypercementosis (Figure 5e–5g). NPP3 was also widely expressed in the tooth and surrounding periodontal tissues, including cementoblasts (Figure 5i–5k). NPP3 is selectively expressed in multiple tissues and cells types in the body, notably in basophils and mast cells.<sup>24,50</sup> Expression and localization of NPP3 in the periodontia were not altered in *Ank*<sup>-/-</sup> or *Enpp1*<sup>-/-</sup> mice compared to WT (Figure 5l–5n). Unlike NPP1, which is selectively expressed in cementoblasts and inducible under conditions of low PP<sub>i</sub> and increased cementogenesis, NPP2 and NPP3 were not altered in compensatory manner.

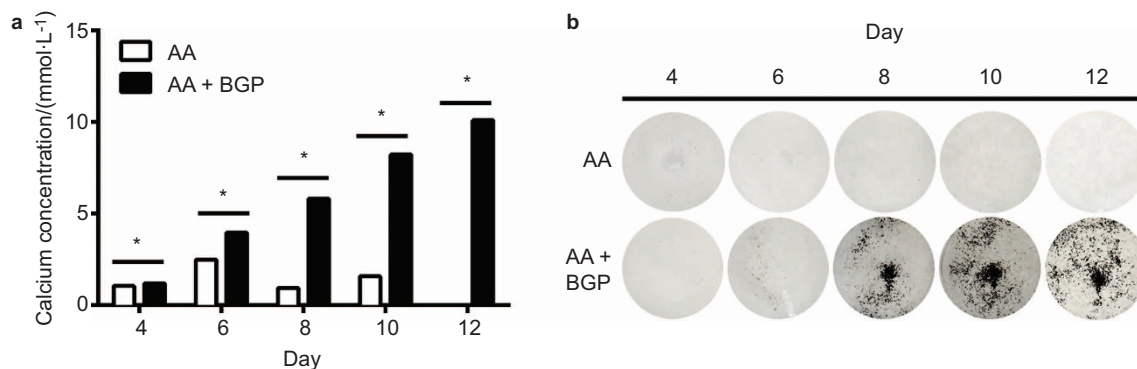
#### Expression of phosphatases in cementum regeneration

Because of the importance of phosphatases TNAP and NPP1 in cementum formation, we aimed to better understand their expression in a model of cementum regeneration. Following surgical removal of cementum from buccal surfaces of the distal root of the first mandibular molar and mesial root of the second molar, tissues were collected for analysis at 1, 15 and 30 days post-surgery.

Expression patterns during regeneration recapitulated the developmental time course. At 1 day post-surgery, loose granulation tissue was observed surrounding the fenestrated root surface (Figure 6a and 6d). No phosphatase expression was noted at this pre-cementum stage; while TNAP was localized to the larger PDL region away from the wound, there was a notable lack of TNAP surrounding the root defect (Figure 6a). By day 15, strong localization of TNAP along the root surface accompanied the formation of new cementum (Figure 6b), and TNAP eventually returned to its normal ubiquitous pattern in the healed PDL by 30 days (Figure 6c). NPP1 was not detectable along the root surface until the advanced time point of 30 days, after new cementum formation was visible (Figure 6d–6f).

#### Regulation of phosphatase expression during cementoblast mineralization *in vitro*

Murine OCCM.30 cementoblasts were cultured *in vitro* to analyze gene expression in relation to matrix mineralization. Cementoblasts cultured under mineralizing conditions with 50 μg·mL<sup>-1</sup> ascorbic acid (AA; required for collagenous matrix deposition) and 10 mmol·mL<sup>-1</sup> BGP (an organic phosphate source) promoted deposition of mineral nodules. Quantitation of calcium in the matrix revealed significantly increased deposition of mineral nodules under mineralizing conditions



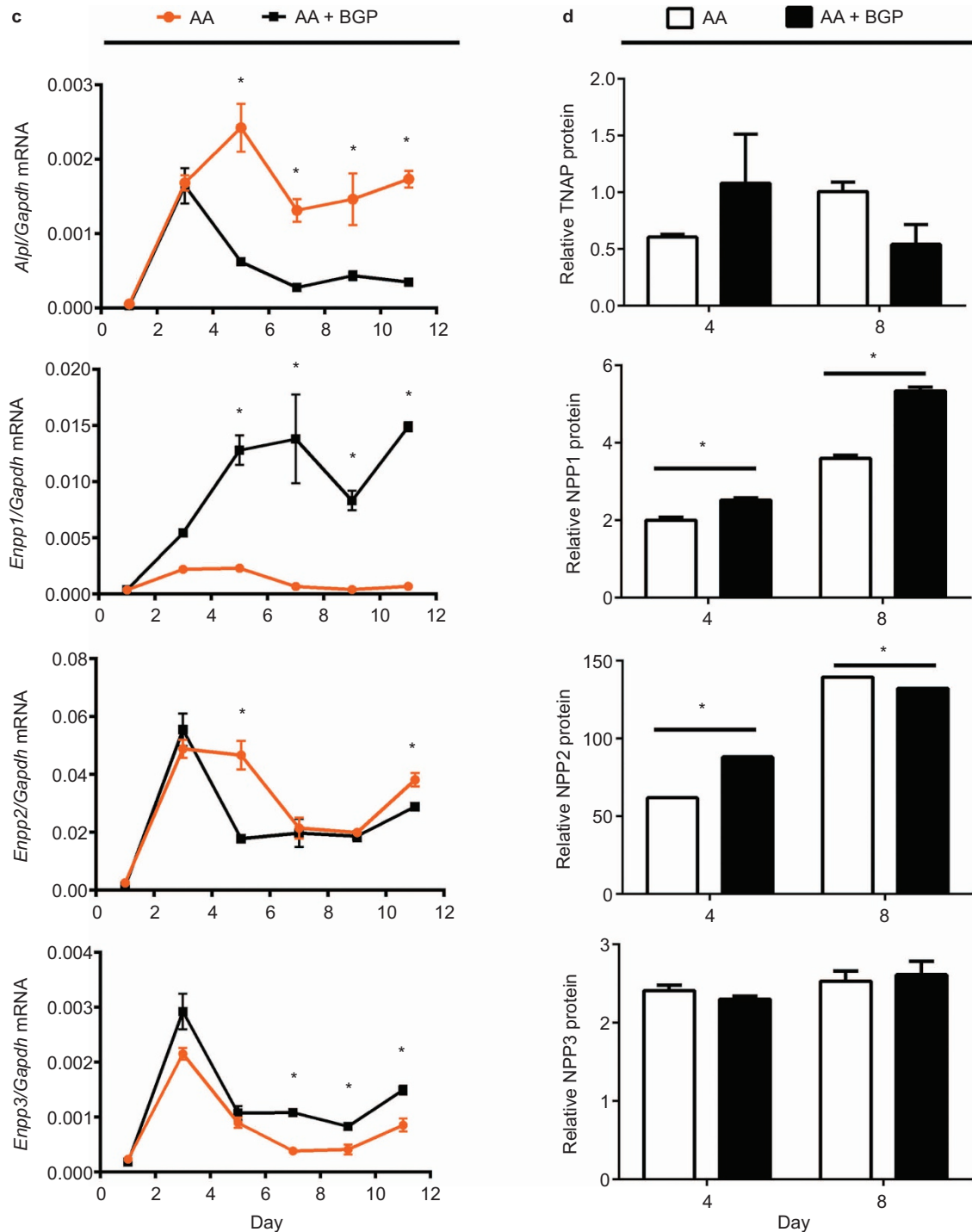


**Figure 7 Regulation of phosphatase expression during cementoblast mineralization *in vitro*.** Murine OCCM.30 cementoblasts were cultured under mineralizing conditions with  $50 \mu\text{g}\cdot\text{mL}^{-1}$  AA and  $10 \text{mmol}\cdot\text{L}^{-1}$  BGP or non-mineralizing conditions (AA only). (a) Mineralizing conditions promote significantly increased calcium deposition on all days (4–12) assayed. (b) von Kossa staining reveals visible mineral nodules under mineralizing conditions by day 6, increasing on later days. (c) Gene expression of phosphatases was assayed by quantitative PCR. *Alpl* expression peaks early (by 3–5 days), then declines for both mineralizing and non-mineralizing conditions, though *Alpl* expression under mineralizing conditions is significantly repressed on days 4–12. Under mineralizing conditions, *Enpp1* mRNA achieves significantly higher concentrations than controls on later days 5–11. *Enpp2* and *3* both peak early on days 3–5, with expression patterns matching between mineralizing and non-mineralizing cells, though some time points exhibit significant differences between treatments. Patterns of *Enpp2* and *3* expression under mineralizing conditions do not match the dramatic upregulation of *Enpp1* mRNA. (d) Cellular protein concentration of phosphatases was assayed by ELISA on days 4 and 8. While TNAP protein is not different in mineralizing vs. non-mineralizing cells, NPP1 protein is significantly increased in cementoblasts in mineralization media at both time points. NPP2 protein exhibits inconsistent changes over the culture period, while NPP3 protein is not significantly different on days 4 and 8. \* indicates significance by Student's (independent samples) *t*-test for  $P < 0.05$ . AA, ascorbic acid; BGP,  $\beta$ -glycerophosphate; ELISA, enzyme linked immunosorbent assay; NPP, nucleotide pyrophosphatase phosphodiesterase; PCR, polymerase chain reaction; TNAP, tissue-nonspecific alkaline phosphatase.

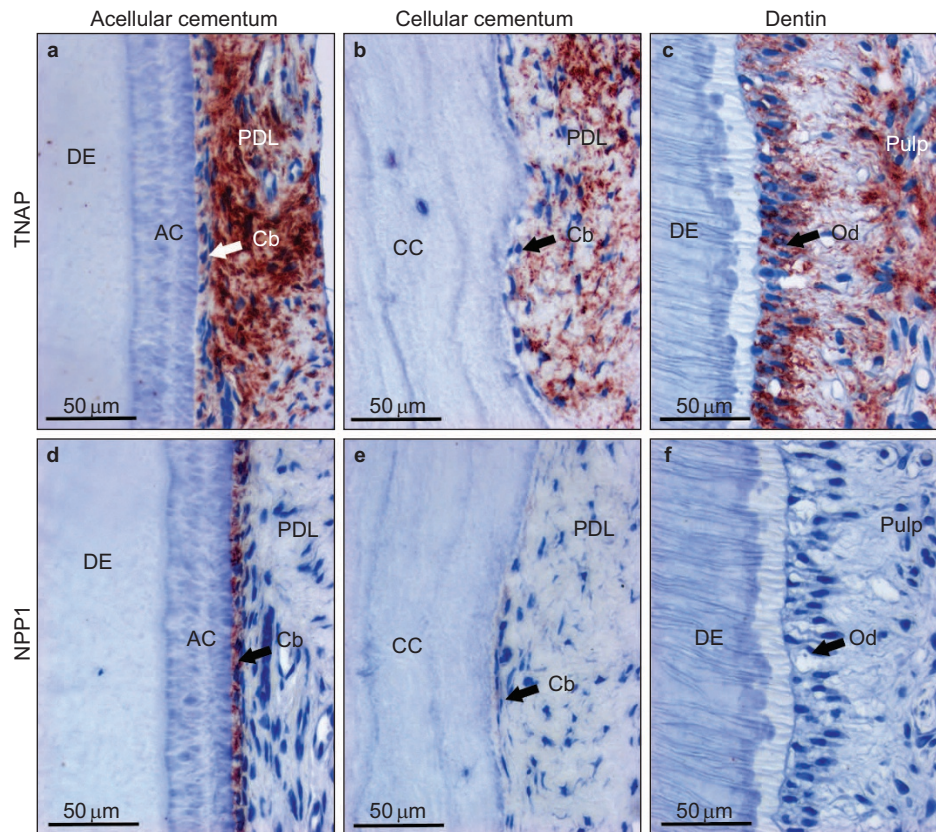


**Figure 8 Expression of TNAP and NPP1 in human teeth.** In an adult human molar tooth, TNAP is found in cells near the root surface as well in the PDL space, for regions of both (a) AC and (b) CC. (c) TNAP is also expressed by odontoblasts lining the DE. (d) The strongest expression of NPP1 in the human molar is found specifically in root-lining cementoblasts of the acellular cementum, while (e) cementoblasts lining the cellular cementum and (f) odontoblasts display low level or no NPP1 localization. AC, acellular cementum; Cb, cementoblast; CC, cellular cementum; DE, dentin; NPP, nucleotide pyrophosphatase phosphodiesterase; Od, odontoblast; PDL, periodontal ligament; TNAP, tissue-nonspecific alkaline phosphatase.

(Figure 7a; AA+BGP vs. AA only), where mineral nodules were visible by von Kossa staining by day 6, and progressively increased on later days (Figure 7b).

Expression of target genes was assayed by quantitative PCR throughout the experiment (Figure 7c). *Alpl* expression peaked early (by 3–5 days), then declined. This was true for both mineralizing and non-mineralizing conditions, though *Alpl* expression under mineralizing conditions was repressed (70%–80%) at later times, consistent with a negative feedback loop (possibly involving  $P_i$  ion production). Under mineralizing conditions, *Enpp1* mRNA achieved significantly higher concentrations than controls (up to 20-fold greater) on later days 5–11, coincident with ongoing mineral accumulation. *Enpp2* and 3 both peaked early on days 3–5, and expression profiles in AA vs. AA+BGP conditions generally matched. Although some time points exhibited significant differences (about twofold or less) in mineralizing vs. nonmineralizing conditions, clear and consistent patterns were not observed over the course of experiments. Notably, patterns of *Enpp2* and *Enpp3* expression under mineralizing conditions did not match the dramatic upregulation of *Enpp1* mRNA.

Because of the gene expression patterns in early (pre-mineralizing) vs. late (post-mineralizing) culture days, ELISA was used to quantify cellular proteins at days 4 (early) and 8 (late) during culture (Figure 7d). While differences in TNAP protein in mineralizing vs. non-mineralizing cells did not reach significance on days 4 and 8, NPP1 was significantly increased (25% and 50%,

respectively) in cementoblasts in mineralization media. NPP2 protein was increased (40%), then decreased (5%) by mineralizing conditions, though fold-change was not great, and NPP3 protein was not significantly different. Overall, differences in NPP2 and three proteins arising from mineralizing conditions or experimental time point were not as consistent or dramatic as induction of NPP1 gene and protein under mineralizing conditions.

#### Expression of TNAP and NPP1 in human teeth

Results from mouse models revealed widespread TNAP expression in the periodontium and restricted NPP1 expression in cementoblasts lining the acellular cementum. Expression patterns in human teeth were analyzed to determine whether the two phosphatases worked in tandem in a similar way. As previously reported in human tissues,<sup>42</sup> TNAP was found in cells near the root surface as well in the PDL space, for regions of both acellular and cellular cementum (Figure 8a and 8b). TNAP was also present in odontoblasts (Figure 8c), as described before in mouse and human tissues.<sup>35–36</sup> Expression of NPP1 has not been analyzed in human teeth previously. As with mouse, strongest expression of NPP1 in human teeth was found in root-lining cementoblasts of the acellular cementum (Figure 8d). Cementoblasts lining the cellular cementum displayed low level or no NPP1 localization, as did odontoblasts (Figure 8e and 8f). Thus, TNAP and NPP1 expression patterns in human teeth parallel those observed in mouse molars.

## DISCUSSION

Proper formation and mineralization of cementum is critical for tooth function. We analyzed the roles of two phosphatases, TNAP and NPP1, in cementogenesis. Though these factors have been studied previously in the context of cementum, careful analysis of developmental expression patterns in combination with targeted ablation models revealed several new and important findings on how these phosphatases work during tooth root mineralization (Supplementary Table S2). Pro-mineralization enzyme TNAP was expressed at the initiation of cementogenesis for both acellular and cellular cementum. While loss of TNAP abolished acellular cementum, an increased but hypomineralized cellular cementum formed. NPP1 was detectable in cementoblasts only after cementum apposition, and was not consistently found around cellular cementum. Loss of NPP1 resulted in a rapidly growing acellular cementum, whereas cellular cementum remained unaltered. These data support carefully orchestrated temporal functions where TNAP is expressed early to initiate cementum mineralization (under low  $PP_i$ ), and NPP1 expression increases after cementum apposition (raising local  $PP_i$ , allowing for tightly controlled acellular cementum growth. This model is presented in Figure 9. NPP1 does not play a major role in cellular cementum apposition. NPP2 and NPP3 do not appear to play important regulatory roles in periodontal formation. Developmental patterns of TNAP and NPP1 were recapitulated in a mouse model for cementum regeneration, and *in vitro* in mineralizing cementoblasts. Here we show for the first time, specific localization of NPP1 to cementoblasts in human teeth, supporting  $PP_i$  regulation as a common mechanism for controlling cementum apposition in the

mouse and human, thus likely a common mechanism across species. These findings confirm  $PP_i$  metabolic machinery as potential targets for pharmacological manipulation to promote acellular cementum regeneration.

### The balance of phosphate and pyrophosphate in directing cementogenesis

The ratio of  $P_i/PP_i$  dictates the mineralization milieu, and this ratio is controlled (in part) at the local level by the phosphatases explored in this paper.<sup>9</sup> TNAP is thought to contribute to skeletal mineralization by reducing local levels of the mineralization inhibitor,  $PP_i$ .<sup>7,12,51–52</sup> TNAP has been localized to the periodontal region,<sup>44,53</sup> with alkaline phosphatase activity positively correlated to cementum thickness.<sup>43</sup> We focused on several unanswered questions about the precise function of TNAP in relation to cementum formation. We confirmed that TNAP is expressed in the periodontal region,<sup>21,43,53–54</sup> and identified TNAP expression specifically in cementoblasts at the time acellular or cellular cementum was initiated on the molar. The localization in acellular cementum-producing cementoblasts was particularly telling, as TNAP was not yet widespread in the dental follicle at that stage. Cementoblasts *in vitro* expressed *Alpl* mRNA and TNAP protein, and its gene expression was regulated by mineralizing conditions, consistent with negative feedback from  $P_i$  production.<sup>19,55</sup>

If TNAP is associated with formation and mineralization of both acellular and cellular cementum formation, then the question remained as to why defects of acellular cementum are reported in cases of HPP, while involvement of cellular cementum is reported as less

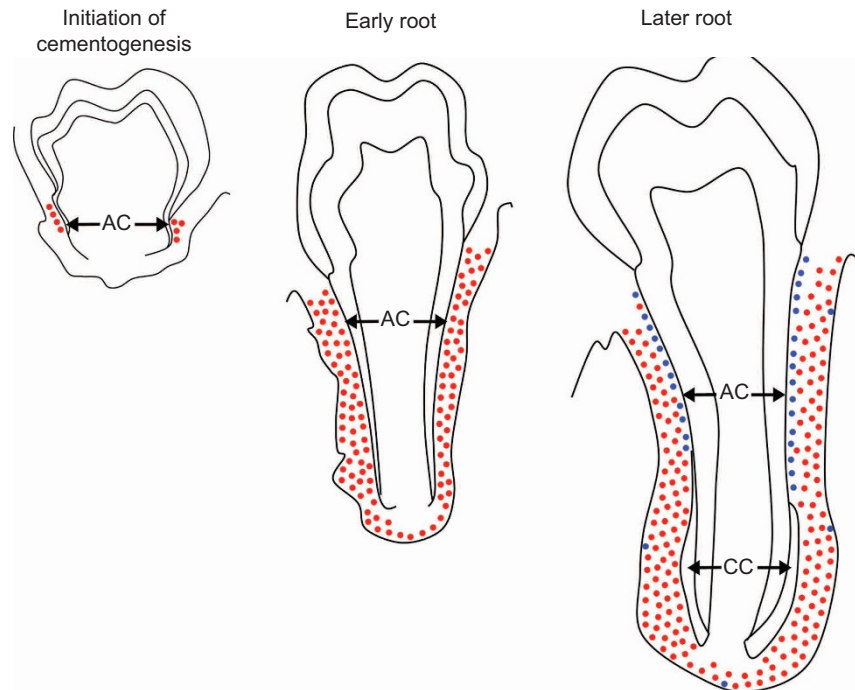


**Figure 9 Phosphatases TNAP and NPP1 regulate tooth root cementogenesis.** This simplified model of tooth root development summarizes TNAP and NPP1 expression in relation to cementum formation (note that enzyme expression in other tissue compartments is not shown here). At initiation of cementogenesis, prominerallizing  $PP_i$  enzyme TNAP (indicated by red dots) is expressed in cementoblasts at sites of AC formation on root dentin, while being absent in the larger dental follicle. During early root formation, when acellular cementum is expanding, TNAP becomes widespread in the PDL region. In later root formation, TNAP is present in PDL and at sites of CC at the apical root, while mineralization limiting enzyme NPP1 (indicated by blue dots) is selectively expressed by cementoblasts bordering the acellular cementum. In this way, acellular cementum apposition is temporally regulated by TNAP (by increasing  $P_i/PP_i$  ratio) and NPP1 (by decreasing  $P_i/PP_i$  ratio). AC, acellular cementum; CC, cellular cementum; NPP, nucleotide pyrophosphatase phosphodiesterase; PDL, periodontal ligament; TNAP, tissue-nonspecific alkaline phosphatase.

affected or unaffected.<sup>16–18,46,56–63</sup> In *Alpl*<sup>-/-</sup> mice, it was revealed that while acellular cementum formation was inhibited, cellular cementum matrix was produced in larger amounts and covered a greater extent of the root surface, going beyond the normal boundary on the tooth apex, albeit in a hypomineralized ‘cementoid’ state. The presence of cellular cementum under HPP conditions may, in part, explain discrepancies in the HPP case literature; though cellular cementum is hypomineralized and with unknown functional competence in the *Alpl*<sup>-/-</sup> mouse, the presence of this tissue on teeth from human subjects could give the impression that cellular cementum was unperturbed in HPP. It is also possible that if cementoid were formed on the roots of human subjects with HPP, that mineralization could be improved given enough time, *i.e.*, a rescue of sorts. This is an aspect that deserves more study to corroborate. It also remains unclear why greater cellular cementum matrix synthesis should occur under HPP conditions. Hypotheses include a functional response of cellular cementum to the poor periodontal attachment of the HPP tooth, or the weakened mechanical status of the tooth when the underlying dentin mineralization is poor. Interestingly, an identical cementoid phenotype resulted in rodents administered 1-hydroxyethylidene-1,1-bisphosphonate, a first generation bisphosphonate that acts as a non-hydrolyzable synthetic PP<sub>i</sub>. 1-hydroxyethylidene-1,1-bisphosphonate inhibited new acellular cementum formation, blocked dentin matrix mineralization and caused an increased production of apically located cementoid.<sup>64–65</sup>

The inverse responses of acellular *versus* cellular cementum to HPP in the mouse underscore the different developmental regulation of these tissues. Acellular cementum depends more directly on the mineralization process, while cellular cementum forms in a more bone-like two-step process of matrix production followed by its mineralization; a sufficient disturbance that delays mineralization of cellular cementum may abolish acellular cementum, effectively destroying PDL attachment.<sup>1,19,37</sup>

The question remains of how acellular cementum remains a slowly growing tissue, in light of the TNAP-rich periodontal environment, and persistent TNAP expression by cementoblasts demonstrated here. We propose that NPP1, in part, helps to answer this question. Developmental analysis revealed definitively that NPP1 expression specifically increases in cementoblasts after acellular cementum is established. Thus, following initiation of acellular cementum under the influence of TNAP (and high P<sub>i</sub>/PP<sub>i</sub> ratio), cementoblasts increase NPP1 expression (reducing the P<sub>i</sub>/PP<sub>i</sub> ratio), and the apposition of acellular cementum is tightly regulated to allow only slow growth over life. Cementoblasts *in vitro* also significantly increased NPP1 gene and protein expression under mineralizing conditions. Additional evidence supports this hypothesis. Reduction of PP<sub>i</sub> by loss-of-function of ANK results in a tooth phenotype identical to that of the *Enpp1*<sup>-/-</sup> mouse, namely rapidly forming and abundant acellular cementum.<sup>19,30,37,66</sup> This means that NPP1 is not solely responsible for this regulatory role; ANK regulates PP<sub>i</sub> transport<sup>31,67</sup> and appears to have a parallel but non-redundant role in controlling acellular cementum.

Results generated here do not support direct roles for the related proteins, NPP2 and NPP3, nor overlapping roles with NPP1. NPP2 and NPP3 have been explored previously for their potential roles in skeletal mineralization.<sup>29,68</sup> While both are reported to have pyrophosphohydrolase activity *in vitro*,<sup>24</sup> further evidence supports different physiological substrates. NPP2 (also known as autotaxin) is a phospholipase D that produces lipid mediator lysophosphatidic acid from lysophospholipids including lysophosphatidylcholine.<sup>49,69–70</sup> NPP3 (also known as CD203c, PD-1β and gp130<sup>RB13-6</sup>) hydrolyzes nucleotide sugars and, and is a marker of activated basophils and mast

cells.<sup>23–24,50,71</sup> While we found that NPP2 and NPP3 are expressed in periodontal tissues, there is a lack of temporal and spatial regulation of expression during root development, and lack of compensation in the face of low PP<sub>i</sub> and hypermineralization in either the *Enpp1*<sup>-/-</sup> or *Ank*<sup>-/-</sup> mice. Moreover, *Enpp2* and *Enpp3* showed inconsistent expression patterns in mineralizing *vs.* non-mineralizing conditions *in vitro*, and early peaks in expression of both factors are consistent with other cellular functions outlined above. Further studies, including knock-out mice or gene silencing, would be necessary to confirm these observations, though *Enpp2*<sup>-/-</sup> mice are embryonic lethal.<sup>72</sup> To date, NPP1 appears to have a unique role in regulating acellular cementum growth (parallel to ANK, as previously discussed). While other factors likely contribute to maintenance of the cementum–PDL border and an unmineralized PDL space (e.g., osteopontin, matrix gla protein and periostin), the dramatic phenotypes of the *Enpp1*<sup>-/-</sup> and *Ank*<sup>-/-</sup> mice identify these as central, non-redundant factors in controlling acellular cementum mineralization.

The mouse incisor featured a slightly different pattern of phosphatase expression than the molar. While TNAP became widespread in the molar periodontium, a clear separation of TNAP from the incisor root surface was noted after acellular cementum was formed. Like the molar, NPP1 was expressed at the incisor root surface following cementum formation. This pattern would be expected to result in lower P<sub>i</sub>/PP<sub>i</sub> ratio and a local environment more restrictive for mineralization. This is interesting in light of several previous observations. While recombinant mineral-targeted TNAP enzyme successfully rescued molar mineralization in the *Alpl*<sup>-/-</sup> mouse, the incisor was more resistant to correction.<sup>35,45,73</sup> Human incisor teeth (which are not continuously erupting) feature predominantly acellular cementum, and are frequently lost under HPP conditions, while back teeth are sometimes maintained, especially in mild to moderate HPP.<sup>15</sup> It is possible that multirooted teeth are better preserved under HPP in part due to cellular cementum–PDL attachment. Important site-specific differences in TNAP, NPP1, and the associated P<sub>i</sub>/PP<sub>i</sub> ratio have been reported before, such as the greater responsiveness of the axial skeleton *versus* the appendicular skeleton to rescue.<sup>9,74</sup>

## CONCLUSIONS AND FUTURE DIRECTIONS

The information gained from these studies provides insights on tooth root development, and may inform therapies to promote cementum regeneration and return to periodontal function. Repair and regeneration of periodontal tissues lost to disease has been achieved using growth and differentiation factors.<sup>75–80</sup> However, the increasing recognition that acellular cementum may be more potently influenced by the P<sub>i</sub>/PP<sub>i</sub> ratio,<sup>19,37</sup> or other mineralization-related factors in the local milieu,<sup>33</sup> should encourage novel therapies directed at regeneration of this tissue. Furthermore, establishing the functional relationships during cementogenesis of TNAP, NPP1 and ANK with other P<sub>i</sub>- and PP<sub>i</sub>-related factors, such as PHOSPHO1,<sup>36,81</sup> CD73 (refs. 82–83) and ABCC6,<sup>84</sup> requires further study and is necessary to more completely understand cementum mineralization. While we have demonstrated increased cementum regeneration resulting from genetic reduction of PP<sub>i</sub> in the *Ank*<sup>-/-</sup> mouse model,<sup>39</sup> similar and parallel pharmacological strategies, such as delivery of TNAP,<sup>45,85</sup> are warranted in additional animal models to confirm the potential of this approach.

## ACKNOWLEDGEMENTS

This research was supported by the Intramural Research Program of the National Institute of Arthritis and Musculoskeletal and Skin Diseases (NIAMS) of the National Institutes of Health (NIH) and extramural NIH funding

(JLM—DE12889 and AR53102). The authors thank Dr Thaisangela Rodrigues for her role in development and execution of the mouse periodontal defect model featured here and in a previous publication.

- 1 Foster BL, Somerman MJ. Cementum/McCauley LK, Somerman MJ eds. *Mineralized tissues in oral and craniofacial science: biological principles and clinical correlates*. Ames: Wiley-Blackwell, 2012: 169–192.
- 2 Foster BL, Popowics TE, Fong HK *et al*. Advances in defining regulators of cementum development and periodontal regeneration. *Curr Top Dev Biol* 2007; **78**: 47–126.
- 3 Bosshardt DD. Are cementoblasts a subpopulation of osteoblasts or a unique phenotype?. *J Dent Res* 2005; **84**(5): 390–406.
- 4 Diekwisch TG. The developmental biology of cementum. *Int J Dev Biol* 2001; **45**(5/6): 695–706.
- 5 Foster BL, Tompkins KA, Rutherford RB *et al*. Phosphate: known and potential roles during development and regeneration of teeth and supporting structures. *Birth Defects Res C Embryo Today* 2008; **84**(4): 281–314.
- 6 McKee MD, Hoac B, Addison WN *et al*. Extracellular matrix mineralization in periodontal tissues: noncollagenous matrix proteins, enzymes, and relationship to hypophosphatasia and X-linked hypophosphatemia. *Periodontology* 2000 2013; **63**(1): 102–122.
- 7 Murshed M, Harmey D, Millán JL *et al*. Unique coexpression in osteoblasts of broadly expressed genes accounts for the spatial restriction of ECM mineralization to bone. *Genes Dev* 2005; **19**(9): 1093–1104.
- 8 Foster BL, Nociti FH Jr, Somerman MJ. The rachitic tooth. *Endocr Rev* 2014; **35**(1): 1–34.
- 9 Millán JL. The role of phosphatases in the initiation of skeletal mineralization. *Calcif Tissue Int* 2013; **93**(4): 299–306.
- 10 Millán JL. *Mammalian alkaline phosphatases: from biology to applications in medicine and biotechnology*. Weinheim: Wiley-VCH, 2006: 337.
- 11 Whyte MP. Hypophosphatasia/Scriver C, Beaudet A, Sly W, Valle D *et al*. eds. *The metabolic and molecular bases of inherited disease*. 8th ed. New York: McGraw-Hill, 2001: 5313–5329.
- 12 Whyte MP. Hypophosphatasia and the role of alkaline phosphatase in skeletal mineralization. *Endocr Rev* 1994; **15**(4): 439–461.
- 13 Fedde KN, Blair L, Silverstein J *et al*. Alkaline phosphatase knock-out mice recapitulate the metabolic and skeletal defects of infantile hypophosphatasia. *J Bone Miner Res* 1999; **14**(12): 2015–2026.
- 14 Narisawa S, Fröhlander N, Millán JL. Inactivation of two mouse alkaline phosphatase genes and establishment of a model of infantile hypophosphatasia. *Dev Dyn* 1997; **208**(3): 432–446.
- 15 Reibel A, Manière MC, Clauss F *et al*. Orodental phenotype and genotype findings in all subtypes of hypophosphatasia. *Orphanet J Rare Dis* 2009; **4**: 6.
- 16 Rodrigues TR, Georgetti AP, Martins L *et al*. Clinical correlate: case study of identical twins with cementum and periodontal defects resulting from odontohypophosphatasia // McCauley LK, Somerman MJ eds. *Mineralized tissues in oral and craniofacial science: biological principles and clinical correlates*. Ames: Wiley-Blackwell, 2012: 183–190.
- 17 Bruckner RJ, Rickles NH, Porter DR. Hypophosphatasia with premature shedding of teeth and aplasia of cementum. *Oral Surg Oral Med Oral Pathol* 1962; **15**: 1351–1369.
- 18 van den Bos T, Handoko G, Niehof A *et al*. Cementum and dentin in hypophosphatasia. *J Dent Res* 2005; **84**(11): 1021–1025.
- 19 Foster BL, Nagatomo KJ, Nociti FH Jr *et al*. Central role of pyrophosphate in acellular cementum formation. *PLoS One* 2012; **7**(6): e38393.
- 20 Beertsen W, VandenBos T, Everts V. Root development in mice lacking functional tissue non-specific alkaline phosphatase gene: inhibition of acellular cementum formation. *J Dent Res* 1999; **78**(6): 1221–1229.
- 21 Gao J, Symons AL, Haase H *et al*. Should cementoblasts express alkaline phosphatase activity? Preliminary study of rat cementoblasts *in vitro*. *J Periodontol* 1999; **70**(9): 951–959.
- 22 Stefan C, Jansen S, Bollen M. NPP-type ectophosphodiesterases: unity in diversity. *Trends Biochem Sci* 2005; **30**(10): 542–550.
- 23 Goding JW, Grobden B, Slegers H. Physiological and pathophysiological functions of the ecto-nucleotide pyrophosphatase/phosphodiesterase family. *Biochim Biophys Acta* 2003; **1638**(1): 1–19.
- 24 Bollen M, Gijsbers R, Ceulemans H *et al*. Nucleotide pyrophosphatases/phosphodiesterases on the move. *Crit Rev Biochem Mol Biol* 2000; **35**(6): 393–432.
- 25 Jansen S, Perrakis A, Ulens C *et al*. Structure of NPP1, an ectonucleotide pyrophosphatase/phosphodiesterase involved in tissue calcification. *Structure* 2012; **20**(11): 1948–1959.
- 26 Harmey D, Hesse L, Narisawa S *et al*. Concerted regulation of inorganic pyrophosphate and osteopontin by AKP2, ENPP1, and ANK: an integrated model of the pathogenesis of mineralization disorders. *Am J Pathol* 2004; **164**(4): 1199–1209.
- 27 Hesse L, Johnson KA, Anderson HC *et al*. Tissue-nonspecific alkaline phosphatase and plasma cell membrane glycoprotein-1 are central antagonistic regulators of bone mineralization. *Proc Natl Acad Sci U S A* 2002; **99**(14): 9445–9449.
- 28 Ruf N, Uhlenberg B, Terkeltaub R *et al*. The mutational spectrum of ENPP1 as arising after the analysis of 23 unrelated patients with generalized arterial calcification of infancy (GACI). *Hum Mutat* 2005; **25**(1): 98.
- 29 Johnson K, Goding J, van Etten D *et al*. Linked deficiencies in extracellular PP, and osteopontin mediate pathologic calcification associated with defective PC-1 and ANK expression. *J Bone Miner Res* 2003; **18**(6): 994–1004.
- 30 Nociti FH Jr, Berry JE, Foster BL *et al*. Cementum: a phosphate-sensitive tissue. *J Dent Res* 2002; **81**(12): 817–821.
- 31 Gurley KA, Chen H, Guenther C *et al*. Mineral formation in joints caused by complete or joint-specific loss of ANK function. *J Bone Miner Res* 2006; **21**(8): 1238–1247.
- 32 Foster BL. Methods for studying tooth root cementum by light microscopy. *Int J Oral Sci* 2012; **4**(3): 119–128.
- 33 Foster BL, Soenjaya Y, Nociti FH Jr *et al*. Deficiency in acellular cementum and periodontal attachment in bsp null mice. *J Dent Res* 2013; **92**(2): 166–172.
- 34 Yadav MC, de Oliveira RC, Foster BL *et al*. Enzyme replacement prevents enamel defects in hypophosphatasia mice. *J Bone Miner Res* 2012; **27**(8): 1722–1734.
- 35 Foster BL, Nagatomo KJ, Tso HW *et al*. Tooth root dentin mineralization defects in a mouse model of hypophosphatasia. *J Bone Miner Res* 2013; **28**(2): 271–282.
- 36 McKee MD, Yadav MC, Foster BL *et al*. Compounded PHOSPHO1/ALPL deficiencies reduce dentin mineralization. *J Dent Res* 2013; **92**(8): 721–727.
- 37 Foster BL, Nagatomo KJ, Bamashmou SO *et al*. The progressive ankylosis protein regulates cementum apposition and extracellular matrix composition. *Cells Tissues Organs* 2011; **194**(5): 382–405.
- 38 King GN, King N, Cruchley AT *et al*. Recombinant human bone morphogenetic protein-2 promotes wound healing in rat periodontal fenestration defects. *J Dent Res* 1997; **76**(8): 1460–1470.
- 39 Rodrigues TL, Nagatomo KJ, Foster BL *et al*. Modulation of phosphate/pyrophosphate metabolism to regenerate the periodontium: a novel *in vivo* approach. *J Periodontol* 2011; **82**(12): 1757–1766.
- 40 D'Errico JA, Berry JE, Ouyang H *et al*. Employing a transgenic animal model to obtain cementoblasts *in vitro*. *J Periodontol* 2000; **71**(1): 63–72.
- 41 Berry JE, Zhao M, Jin Q *et al*. Exploring the origins of cementoblasts and their trigger factors. *Connect Tissue Res* 2003; **44**(Suppl 1): 97–102.
- 42 van den Bos T, Beertsen W. Alkaline phosphatase activity in human periodontal ligament: age effect and relation to cementum growth rate. *J Periodont Res* 1999; **34**(1): 1–6.
- 43 Groeneveld MC, Everts V, Beertsen W. Alkaline phosphatase activity in the periodontal ligament and gingiva of the rat molar: its relation to cementum formation. *J Dent Res* 1995; **74**(7): 1374–1381.
- 44 Groeneveld MC, Everts V, Beertsen W. A quantitative enzyme histochemical analysis of the distribution of alkaline phosphatase activity in the periodontal ligament of the rat incisor. *J Dent Res* 1993; **72**(9): 1344–1350.
- 45 McKee MD, Nakano Y, Masica DL *et al*. Enzyme replacement therapy prevents dental defects in a model of hypophosphatasia. *J Dent Res* 2011; **90**(4): 470–476.
- 46 Hu JC, Plaetke R, Mornet E *et al*. Characterization of a family with dominant hypophosphatasia. *Eur J Oral Sci* 2000; **108**(3): 189–194.
- 47 Ho SP, Senkyrikova P, Marshall GW *et al*. Structure, chemical composition and mechanical properties of coronal cementum in human deciduous molars. *Dent Mater* 2009; **25**(10): 1195–1204.
- 48 Groeneveld MC, Everts V, Beertsen W. Formation of afibrillar acellular cementum-like layers induced by alkaline phosphatase activity from periodontal ligament explants maintained *in vitro*. *J Dent Res* 1994; **73**(10): 1588–1592.
- 49 Nakanaga K, Hama K, Aoki J. Autotaxin—an LPA producing enzyme with diverse functions. *J Biochem* 2010; **148**(1): 13–24.
- 50 Bühring HJ, Streble A, Valent P. The basophil-specific ectoenzyme E-NPP3 (CD203c) as a marker for cell activation and allergy diagnosis. *Int Arch Allergy Immunol* 2004; **133**(4): 317–329.
- 51 Millán JL. Alkaline phosphatases: structure, substrate specificity and functional relatedness to other members of a large superfamily of enzymes. *Purinergic Signal* 2006; **2**(2): 335–341.
- 52 Addison WN, Azari F, Sørensen ES *et al*. Pyrophosphate inhibits mineralization of osteoblast cultures by binding to mineral, up-regulating osteopontin, and inhibiting alkaline phosphatase activity. *J Biol Chem* 2007; **282**(21): 15872–15883.
- 53 Groeneveld MC, van den Bos T, Everts V *et al*. Cell-bound and extracellular matrix-associated alkaline phosphatase activity in rat periodontal ligament. Experimental Oral Biology Group. *J Periodont Res* 1996; **31**(1): 73–79.
- 54 Rooser SM, Liu B, Helms JA. Role of Wnt signaling in the biology of the periodontium. *Dev Dyn* 2010; **239**(1): 140–147.
- 55 Foster BL, Nociti FH Jr, Swanson EC *et al*. Regulation of cementoblast gene expression by inorganic phosphate *in vitro*. *Calcif Tissue Int* 2006; **78**(2): 103–112.
- 56 Wei KW, Xuan K, Liu YL *et al*. Clinical, pathological and genetic evaluations of Chinese patients with autosomal-dominant hypophosphatasia. *Arch Oral Biol* 2010; **55**(12): 1017–1023.
- 57 Hu JC, Simmer JP. Developmental biology and genetics of dental malformations. *Orthod Craniofac Res* 2007; **10**(2): 45–52.
- 58 Olsson A, Mattson L, Blomquist HK *et al*. Hypophosphatasia affecting the permanent dentition. *J Oral Pathol Med* 1996; **25**(6): 343–347.
- 59 Plagmann HC, Kocher T, Kuhrau N *et al*. Periodontal manifestation of hypophosphatasia. A family case report. *J Clin Periodontol* 1994; **21**(10): 710–716.
- 60 Chapple IL. Hypophosphatasia: dental aspects and mode of inheritance. *J Clin Periodontol* 1993; **20**(9): 615–622.
- 61 el-Labban NG, Lee KW, Rule D. Permanent teeth in hypophosphatasia: light and electron microscopic study. *J Oral Pathol Med* 1991; **20**(7): 352–360.
- 62 Macfarlane JD, Swart JG. Dental aspects of hypophosphatasia: a case report, family study, and literature review. *Oral Surg Oral Med Oral Pathol* 1989; **67**(5): 521–526.

- 63 Baab DA, Page RC, Ebersole JL *et al*. Laboratory studies of a family manifesting premature exfoliation of deciduous teeth. *J Clin Periodontol* 1986; **13**(7): 677–683.
- 64 Takano Y, Sakai H, Watanabe E *et al*. Possible role of dentin matrix in region-specific deposition of cellular and acellular extrinsic fibre cementum. *J Electron Microsc (Tokyo)* 2003; **52**(6): 573–580.
- 65 Beertsen W, Niehof A, Everts V. Effects of 1-hydroxyethylidene-1,1-bisphosphonate (HEBP) on the formation of dentin and the periodontal attachment apparatus in the mouse. *Am J Anat* 1985; **174**(1): 83–103.
- 66 Fong H, Foster BL, Sarikaya M *et al*. Structure and mechanical properties of Ank/Ank mutant mouse dental tissues—an animal model for studying periodontal regeneration. *Arch Oral Biol* 2009; **54**(6): 570–576.
- 67 Ho AM, Johnson MD, Kingsley DM. Role of the mouse ank gene in control of tissue calcification and arthritis. *Science* 2000; **289**(5477): 265–270.
- 68 Vaingankar SM, Fitzpatrick TA, Johnson K *et al*. Subcellular targeting and function of osteoblast nucleotide pyrophosphatase phosphodiesterase 1. *Am J Physiol, Cell Physiol* 2004; **286**(5): C1177–C1187.
- 69 Perrakis A, Moolenaar WH. Autotaxin: structure–function and signaling. *J Lipid Res* 2014; **55**(6): 1010–1018.
- 70 Yuelling LM, Fuss B. Autotaxin (ATX): a multi-functional and multi-modular protein possessing enzymatic lysoPLD activity and matricellular properties. *Biochim Biophys Acta* 2008; **1781**(9): 525–530.
- 71 Korekane H, Park JY, Matsumoto A *et al*. Identification of ectonucleotide pyrophosphatase/phosphodiesterase 3 (ENPP3) as a regulator of N-acetylglucosaminyltransferase GnT-IX (GnT-Vb). *J Biol Chem* 2013; **288**(39): 27912–27926.
- 72 Fotopoulou S, Oikonomou N, Grigorieva E *et al*. ATX expression and LPA signalling are vital for the development of the nervous system. *Dev Biol* 2010; **339**(2): 451–464.
- 73 Millán JL, Narisawa S, Lemire I *et al*. Enzyme replacement therapy for murine hypophosphatasia. *J Bone Miner Res* 2008; **23**(6): 777–787.
- 74 Anderson HC, Harmey D, Camacho NP *et al*. Sustained osteomalacia of long bones despite major improvement in other hypophosphatasia-related mineral deficits in tissue nonspecific alkaline phosphatase/nucleotide pyrophosphatase phosphodiesterase 1 double-deficient mice. *Am J Pathol* 2005; **166**(6): 1711–1720.
- 75 Fritz U. Systematic review of the use of growth factors in periodontal regeneration. *J Orofac Orthop* 2012; **73**(6): 425–429.
- 76 Stavropoulos A, Wikesjö UM. Growth and differentiation factors for periodontal regeneration: a review on factors with clinical testing. *J Periodont Res* 2012; **47**(5): 545–553.
- 77 Chen FM, Jin Y. Periodontal tissue engineering and regeneration: current approaches and expanding opportunities. *Tissue Eng Part B Rev* 2010; **16**(2): 219–255.
- 78 Bosshardt DD, Sculean A. Does periodontal tissue regeneration really work? *Periodontology 2000* 2009; **51**: 208–219.
- 79 Taut AD, Jin Q, Chung JH *et al*. Sclerostin antibody stimulates bone regeneration after experimental periodontitis. *J Bone Miner Res* 2013; **28**(11): 2347–2356.
- 80 Darby IB, Morris KH. A systematic review of the use of growth factors in human periodontal regeneration. *J Periodontol* 2013; **84**(4): 465–476.
- 81 Yadav MC, Simão AM, Narisawa S *et al*. Loss of skeletal mineralization by the simultaneous ablation of PHOSPHO1 and alkaline phosphatase function: a unified model of the mechanisms of initiation of skeletal calcification. *J Bone Miner Res* 2011; **26**(2): 286–297.
- 82 St Hilaire C, Ziegler SG, Markello TC *et al*. NT5E mutations and arterial calcifications. *N Engl J Med* 2011; **364**(5): 432–442.
- 83 Markello TC, Pak LK, St Hilaire C *et al*. Vascular pathology of medial arterial calcifications in NT5E deficiency: implications for the role of adenosine in pseudoxanthoma elasticum. *Mol Genet Metab* 2011; **103**(1): 44–50.
- 84 Jansen RS, Küçükosmanoglu A, de Haas M *et al*. ABCC6 prevents ectopic mineralization seen in pseudoxanthoma elasticum by inducing cellular nucleotide release. *Proc Natl Acad Sci U S A* 2013; **110**(50): 20206–20211.
- 85 Osathanon T, Giachelli CM, Somerman MJ. Immobilization of alkaline phosphatase on microporous nanofibrous fibrin scaffolds for bone tissue engineering. *Biomaterials* 2009; **30**(27): 4513–4521.



This work is licensed under a Creative Commons Attribution-NonCommercial-NoDerivs 3.0 Unported License. The images or other third party material in this article are included in the article's Creative Commons license, unless indicated otherwise in the credit line; if the material is not included under the Creative Commons license, users will need to obtain permission from the license holder to reproduce the material. To view a copy of this license, visit <http://creativecommons.org/licenses/by-nc-nd/3.0/>

Supplementary Information for this article can be found on *International Journal of Oral Science's* website (<http://www.nature.com/ijos>).